



Reanalysis of a Cold Surge in Brazil in 1953

Marcelo Zamuriano*, Noemi Imfeld, Stefan Hunziker, Reto Peier, and Giacomo Santi

Oeschger Centre for Climate Change Research and Institute of Geography, University of Bern, Switzerland

Abstract

In the second half of 1953 coffee prices exploded demonstrably due to several cold surges in the coffee growing areas of southern and south-eastern Brazil during wintertime. The cold surge of 5 July 1953 has been graded as an extreme frost event with measured minimum temperature of -0.1°C in São Paulo, but no measurements are available for the coffee growing region to the south-west. Reanalyses such as version 2c of the “Twentieth Century Reanalysis” (20CRv2c) provide an opportunity to study extent, evolution and synoptic conditions of the event. 20CRv2c shows the movement of a cold core anticyclone towards South America and its deflection and advection of cold air equator-wards. However, cold air in 20CRv2c does not reach São Paulo, likely due to erroneous surface pressure observations. Only the reanalysis NCEP/NCAR with assimilated upper-air temperature reaches surface temperature values that are similarly low as observations.

1. Introduction

Freezing weather in southern and south-eastern Brazil is mainly caused by outbreaks of polar air during austral winter (May-August) leading to below-average temperatures that may occasionally extend up to the tropical regions. These so-called “friagems” can severely affect the harvest of agricultural production of south-eastern Brazil (Marengo, 1997). The cold surge event of July 1953 produced intense damage in the coffee growing areas of southern and south-eastern Brazil (Marshall, 1983). As the area used to provide up to 30% of the international coffee production, the loss in harvest contributed to the rise of global coffee prizes by 1954 to a local maximum (Fig. 1).

* Corresponding author: Marcelo Zamuriano, University of Bern, Institute of Geography, Hallerstr. 12, CH-3012 Bern, Switzerland. E-mail: marcelo.zamuriano@giub.unibe.ch

“Friagems” are not rare, they occur year round with a one to two week-frequency during winter, but only occasionally cold air reaches as far as southeastern Brazil or the Amazon region (Sprenger et al., 2013). While summertime incursions enhance convection and rainfall, wintertime cold air incursions mainly affect temperature and may lead to frost (Garreaud, 2000). For the period 1950 to 2000, six extreme cold surges with frost occurrence ($T < 0\text{ }^{\circ}\text{C}$) and 15 strong cold surges with frost occurrence ($0\text{ }^{\circ}\text{C} \leq T \leq 2.5\text{ }^{\circ}\text{C}$) have been registered in São Paulo (Pezza and Ambrizzi, 2005).

Cold surges have a characteristic synoptic-scale pattern influenced by the channelling effect of the Andes and the extension of sea ice cover during austral winter. At middle and upper levels a mid-latitude wave with a ridge to the west of the Pacific coast and a trough extending to the subtropics is present (advecting anticyclonic vorticity to the east of the Andes). At lower levels a strong anticyclone is present to the west of Chile and a cyclone over the South Atlantic. The transient cold core high pressure centre moves onto the southern tip of South America from the Pacific Ocean, intensifies while crossing Argentina two to three days later and transporting large cold air masses towards the Equator (Pezza and Ambrizzi, 2005).

The cold surge of July 1953 has not been studied in detail, as barely any observational records are available. We examine the cold surge development using the version 2c of the “Twentieth Century Reanalysis” (20CRv2c, Compo et al., 2011) and compare it to three other reanalysis datasets. Section 2 describes these datasets and introduces the methods, Section 3 shows the results of our analysis and in Section 4 we discuss our results. A short conclusion is drawn in Section 5.

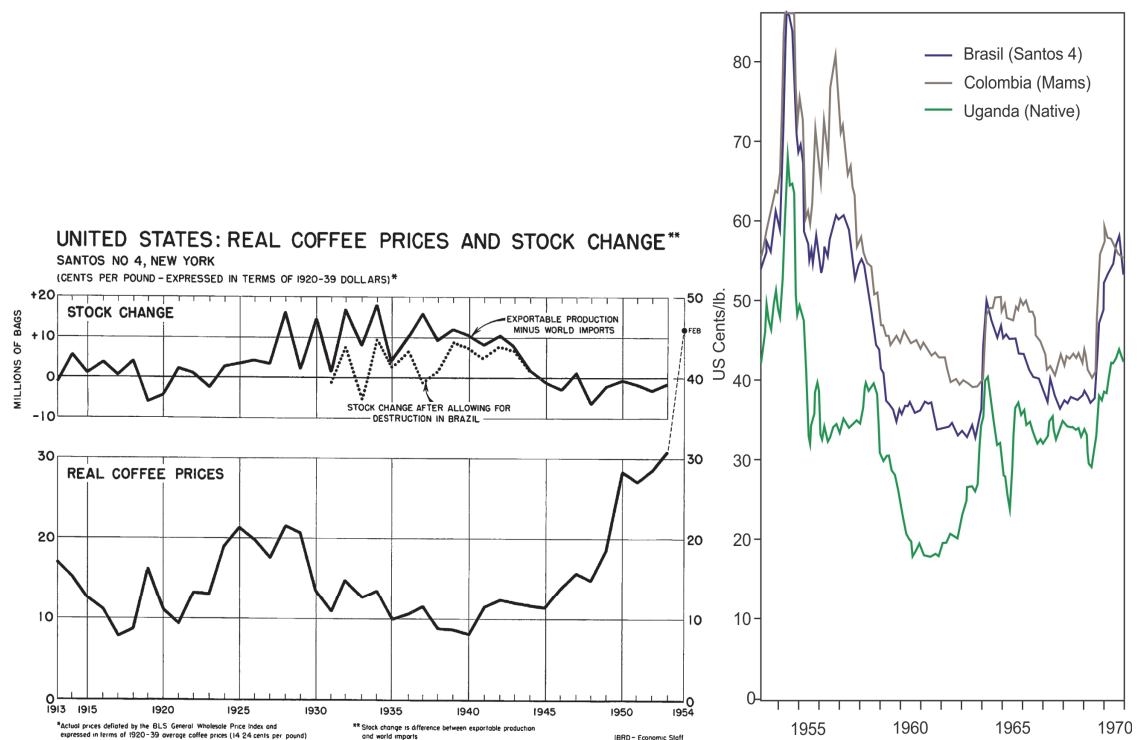


Figure 1. (left) Price of the coffee “Santos 4” in New York from 1913 to early 1954 (from a contemporary memorandum; World Bank, 1954). (right) Coffee price development from the 1950s to 1970 (from Kohlhepp, 1975). The scale is approximately the same.

2. Data and Methods

We compare surface temperatures derived from four reanalysis datasets. 20CRv2c provides a comprehensive global three-dimensional atmospheric dataset spanning a period from 1851 to 2010. It is generated by assimilating surface and sea-level pressure using an Ensemble Kalman Filter method into the CFS model (Saha et al. 2010), which is driven by monthly sea-surface temperatures and sea-ice distributions as boundary conditions (Giese et al., 2016; Hirahara et al., 2014). For the year 1953, the number of assimilated observations over South America is very low. Surface pressure data are only available for some locations along the coast of the continent and from ships north of South America (Fig. 2). Thus, the reanalysis data mainly arise from the model and adjustments due to assimilation are expected to be minor. A unique feature of the 20CRv2c is that it allows an estimate of uncertainty by providing a 56-member ensemble (for details Brönnimann, 2017). The global atmospheric reanalysis has a six-hourly forecast cycle and a $2^\circ \times 2^\circ$ latitude-longitude spatial resolution.

Further, we compare time series from 20CRv2c to the reanalyses NCEP/NCAR (Kistler et al., 2001), ERA-20C (Poli et al., 1996) and CERA-20C (Laloyaux et al., 2016, 2017). ERA-20C is the first ECMWF reanalysis spanning the 20th century from 1900 to 2010. In contrast to 20CRv2c, ERA-20C is a single member reanalysis that assimilates surface pressure and surface winds over the ocean using a 4D-VAR assimilation scheme, but no upper-air and satellite data (Poli et al., 2016). It has a spatial resolution of 125 km and 3-hourly output data. CERA-20C is a ten member coupled ocean-atmosphere reanalysis spanning from 1901 to 2010. In addition to surface pressure and marine wind observations, it as well assimilates ocean temperature and salinity profiles (Laloyaux et al., 2017). The NCEP/NCAR reanalysis provides data for the period 1948 to 2017 with a spatial resolution of

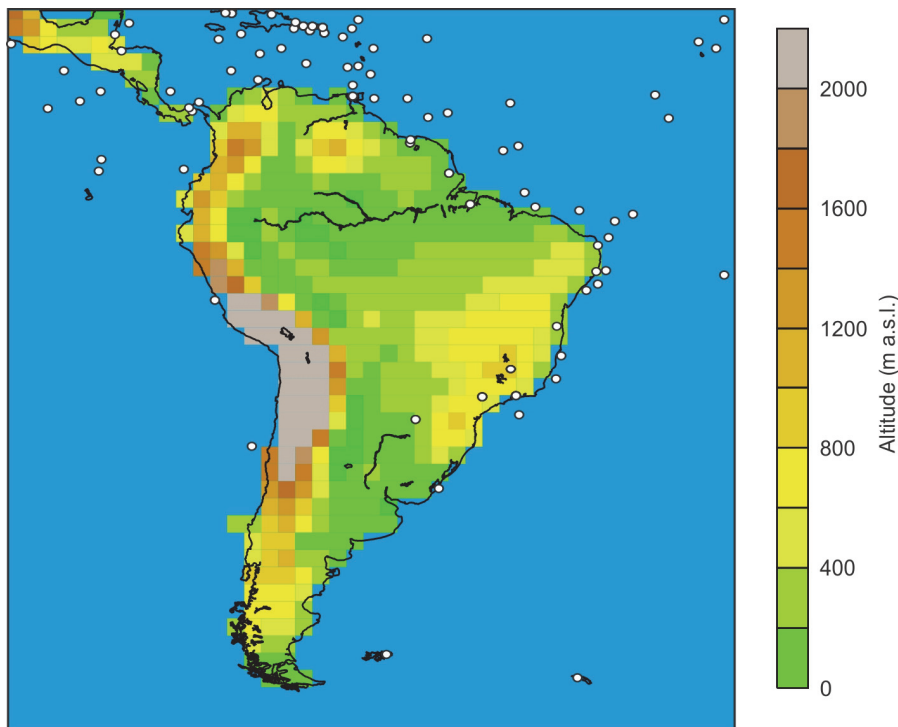


Figure 3. Topography and location of assimilated surface pressure data in 20CRv2c for the analysis of 5 July 1953, 6 UTC. Only very few data for the South American continent is available. Most observations come from ship measurements.

2.5° degrees. It uses spectral statistical interpolation (a 3D-VAR assimilation scheme) with radiosonde data, station data, aircraft and satellite retrievals as input data. It is the longest running reanalysis using radiosonde data and provides data up to date, but its data assimilation scheme and model are rather antiquated (Kalnay et al., 1996). Further details on all data sets used in this book are given in the introductory paper (Brönnimann, 2017).

Indicators used in the present article are daily minimum temperature at 2 m altitude (i.e., the minimum of 6-hourly analyses over a day), sea-level pressure, geopotential height at 500 hPa and wind speed and direction at 995 hPa (note that the latter is calculated from the ensemble mean u and v components of the reanalysis). Analyses are made for the period from 2 to 8 July 1953. For 20CRv2c and NCEP/NCAR we also show anomalies based on the normal period of 1931 to 1960. We denote 5 July 1953 as day 0 following the measurements in São Paulo (Pezza and Ambrizzi, 2005). For the analyses of 20CRv2c we show the ensemble mean and spread (i.e., standard deviation), and for CERA-20C ensemble member statistics are also shown in the comparison among the reanalyses. Particular attention is given to the location with measurements (São Paulo), the coffee growing area (Londrina) and a grid point closer to the Andes (example location).

3. Results

3.1. Two-metre temperature anomalies in 20CRv2c

Daily minimum temperature in 20CRv2c show the northward movement of the cold air incursion up to the western Amazon region in the course of the period from 2 to 9 July (Fig. 3). A slightly negative anomaly is present at day -3 west of São Paulo. This anomaly amplifies strongly from day -1 to day 0, but strong negative temperature anomalies reach neither Londrina nor São Paulo. The strongest temperature anomalies occur on day +2 in the Bolivian lowlands. By day +4 the cold air anomalies have disappeared largely. Temperature anomalies over the Atlantic east of Argentina are negative throughout day -3 to day 0 and they start to increase slowly after day 0.

The spread of temperature anomalies is in general higher over land and particularly over the Andes than over the ocean surface. The spread is highest around the area of strongest cold anomalies, i.e., the area of the cold air outbreak. At day +2 to day +4 this is well visible, indicating that the members differ substantially in the representation of the strength and extent of the cold air outbreak.

3.2. Movement of trough-ridge system in 20CRv2c

The distinctive atmospheric circulation pattern of a cold surge is nicely visible throughout day -3 until day +4 in the surface pressure, wind and geopotential height field (Fig. 4). A cold core high-pressure system is located in front of the Chilean coast, extending towards the eastern coast of the continent on day -3. On day -2 pressure increases above Argentina and a northward movement starts at day -1. At the same time, we observe a system of lower pressure in front of the south Brazilian coast. At day -1 and day 0 southern winds prevail along the Andean mountain chain up to Bolivia. These winds reduce in strength at day +1 and the cold core high pressure systems moves off the coast along with the trough visible in the geopotential height.

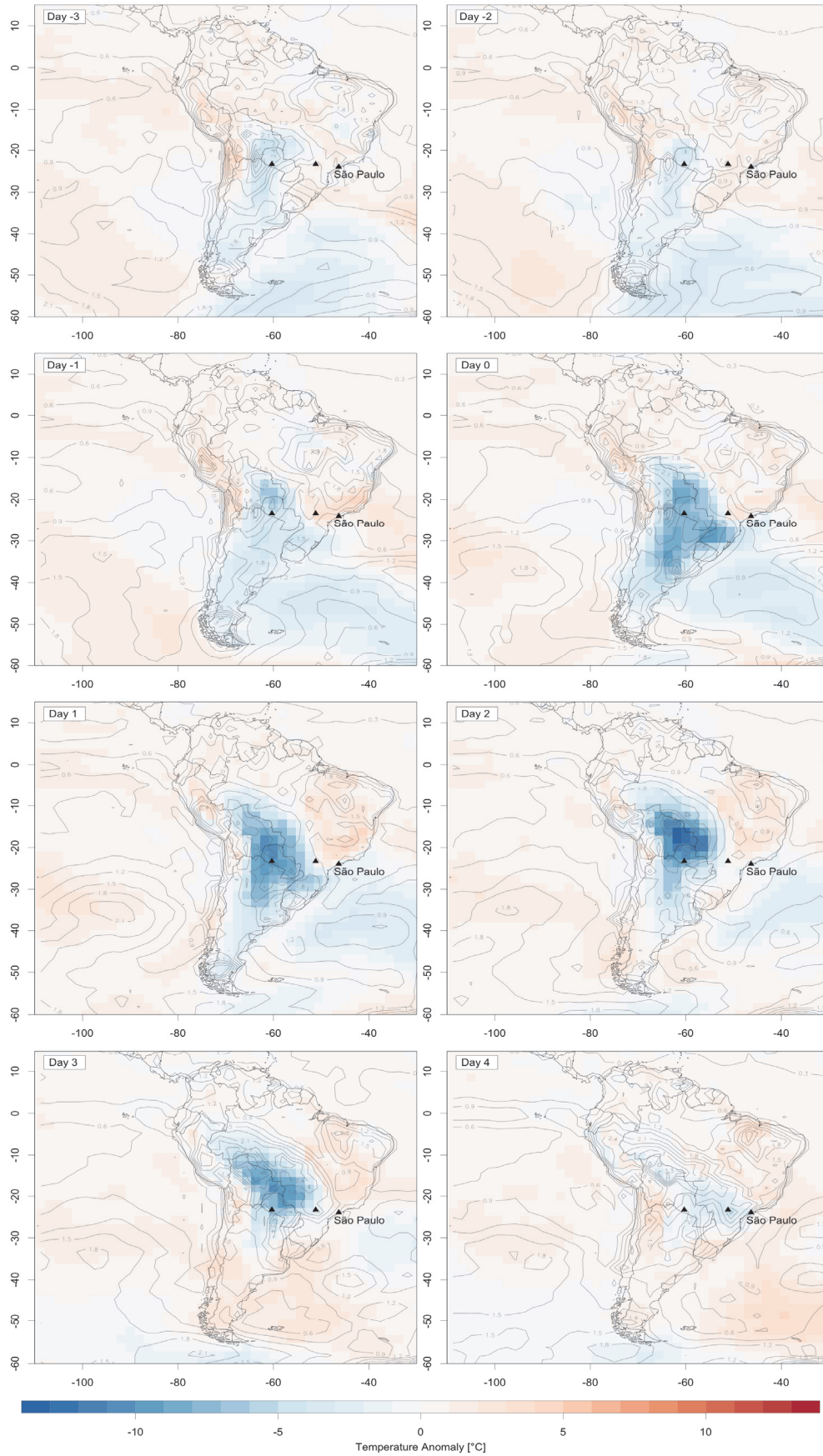


Figure 3. Ensemble mean (colour) and spread (contours) of anomalies of air temperature at two metres for the period from 2 July (day -3) to 9 July (day +4) from 20CRv2c. Anomalies are calculated relative to the 1931 to 1960 period. The three points show São Paulo, Londrina (middle) and a third example location (left).

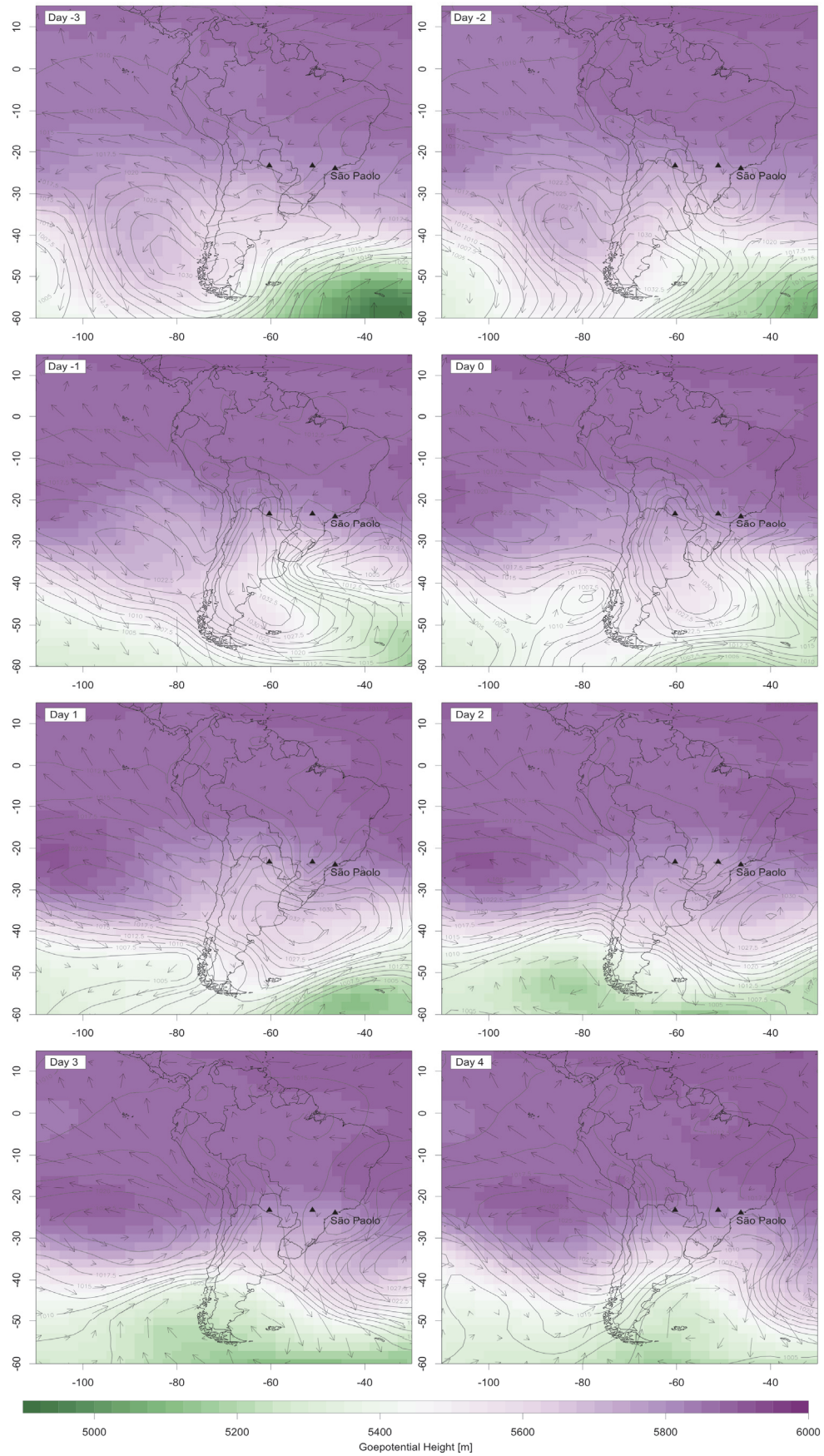


Figure 4. Ensemble mean of anomalies of geopotential height at 500hPa (colour), sea-level pressure (contours) and wind at 995hPa (arrows) for the period from 2 July (day -3) to 9 July (day +4) at 18 UTC for 20CrV2c. The three points show São Paulo, Londrina (middle) and a third example location (left).

3.3. Comparison to other reanalyses

As 20CRv2c does not show the expected low temperature values in the area of Londrina, around 23° S and 51° W, we compare 20CRv2c two-metre temperature to three other reanalyses (Fig. 5). NCEP/NCAR is the only dataset where temperature values drop close to what has been measured in Sao Paulo (1.2°C). As this reanalysis assimilates also upper-air temperatures, this temperature information might be the reason for the values close to observations (Fig. 5a). A second cold surge has been observed in São Paulo on 11 July. This weaker cold surge is as well visible in NCEP/NCAR, whereas the spread for this cold surge in CERA-20C is very high, indicating that some members are able to reproduce the low temperatures in the temperature field. 20CRv2c shows a slight but lagged decrease in temperature. At a grid point further to the west all reanalysis show a decrease with ERA-20C slightly earlier (dashed line).

Together with the abrupt drop in temperatures, a cold surge produces an increase in air pressure (Fig. 5b). For Londrina, all reanalyses show this increase, whereas 20CRv2c shows a lagged and weaker increase. The air pressure time series from 20CRv2c for July does not match the other reanalyses since its variability is much lower. To the west of Londrina, at 60° W, 20CRv2c coincides again with the other reanalyses. All reanalyses agree very well in their pressure fields, as to be expected due to assimilated surface pressure observations in all datasets.

A composite of minimum temperatures from NCEP/NCAR for 5 to 7 July (at 12 UTC) confirms that 20CRv2c may have difficulties in representing the eastward extent of the cold air incursion. Minimum temperatures in NCEP/NCAR reach further east and also extend towards northeast.

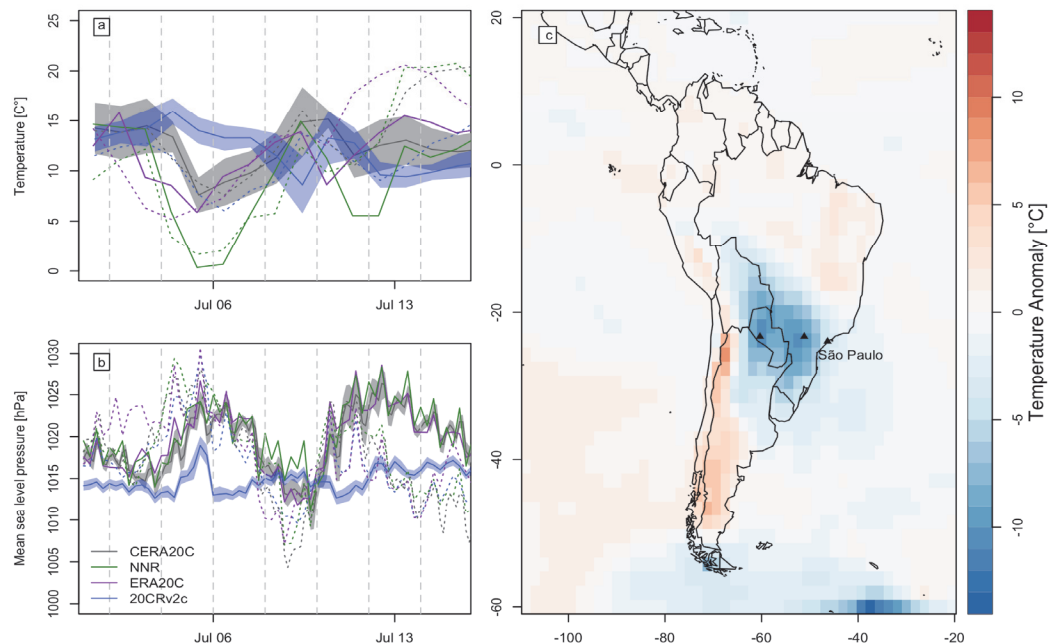


Figure 5. Time series of (a) 2-m temperature and (b) sea-level pressure for the four reanalyses (for 20CRv2c and CERA-20C, ensemble mean and range are given). Solid: 23° S/ 51° W (Londrina), dashed 23° S/ 60° W. (c) Composite from 5–7 July 2017 of NCEP/NCAR minimum temperature anomalies at 12 UTC and locations of São Paulo, Londrina (middle) and grid point visualized as dashed lines in (a) and (b).

4. Discussion

The analysed data confirms that the low temperatures measured in São Paulo in July 1953 are the result of cold air advection from a migratory cold-core anticyclone moving from the South Pole onto South America and extending along the eastern flanks of the Andes northwards. According to the temperature fields in 20CRv2c and NCEP/NCAR, the cold surge reaches up to tropical South America; but the eastward extension differs in these two datasets. The spread of the 56 members from 20CRv2c is increased around the boundaries of the cold air, indicating that the members differ in the extent and strength of the cold air outbreak. To study the spatial extent of the cold surge, it is important to study also the reanalyses ERA-20C and CERA-20C more thoroughly. Time series help visualizing the differences between the reanalyses at the location of Londrina. At this location, 20CRv2c does neither depict a pressure increase nor a temperature drop, even though it is located in an area where pressure observations are assimilated. The low variability and low increase during the cold surge in the mean sea-level pressure time series compared to other reanalyses may indicate a model bias. That seems to be confirmed by the mean sea-level pressure of 20CRv2c that shows a bulb of higher pressure at day -1 and again an isolated area of higher pressure at day +3. Nevertheless, the pressure evolution of the extreme event over the major part of the continent in 20CRv2c resembles the conceptual model for a cold surge evolution over South America proposed by Pezza and Ambrizzi (2005) with a migratory anticyclone.

5. Conclusions

We studied the cold air incursion of 5 July in Southern Brazil using the 20CRv2c reanalysis and compared the results to other reanalysis products available for this time period. The successions of cold air incursions in winter 1953 play a big role in the drop of coffee prices at the world market at end of 1953. For the most affected region, 20CRv2c does not show a dramatic reduction in temperature and its pressure evolution does not fully agree with other reanalyses. We expect this location not to be reliable due to several reasons. Further to the west, we find in all four reanalyses a sudden drop in temperature and the associated jump in mean sea-level pressure. The NCEP/NCAR reanalysis is closest to observations, most likely due to the upper-air temperature observations assimilated in this reanalysis.

The synoptic-scale characteristics of a cold surge are well represented in 20CRv2c with a cold core high-pressure system moving from the Pacific towards the tip of the South American continent and extending towards the tropics east of the Andes. However, the exact spatial extent of this cold surge cannot be derived from the 20CRv2c reanalysis.

Acknowledgements

The Twentieth Century Reanalysis Project dataset was obtained courtesy of the NOAA/OAR/ESRL PSD, Boulder, Colorado, USA, from their web page at <http://www.esrl.noaa.gov/psd/>. Support for the 20CR dataset is provided by the U.S. Department of Energy, Office of Science Innovative and Novel Computational Impact on Theory and Experiment program, Office of Biological and Environmental Research and by the National Oceanic and Atmospheric Administration Climate Program Office. The work was supported by FP7 project ERA-CLIM2, H2020 project EUSTACE, the Swiss National Science Foundation project EXTRA-LARGE and the SNF/R4D project DECADE.

References

- Brönnimann, S. (2017) Weather Extremes in an Ensemble of Historical Reanalyses. In: Brönnimann, S. (Ed.) *Historical Weather Extremes in Reanalyses*. Geographica Bernensia G92, p. 7-22, DOI: 10.4480/GB2017.G92.01.
- Compo, G. P., J. S. Whitaker, P. D. Sardeshmukh, N. Matsui, R. J. Allan, X. Yin, B. E. Gleason, R. S. Vose, G. Rutledge, P. Bessemoulin, S. Brönnimann, M. Brunet, R. I. Crouthamel, A. N. Grant, P. Y. Groisman, P. D. Jones, M. Kruk, A. C. Kruger, G. J. Marshall, M. Maugeri, H. Y. Mok, Ø. Nordli, T. F. Ross, R. M. Trigo, X. Wang, S. D. Woodruff, and S. J. Worley (2011) The Twentieth Century Reanalysis Project. *Q. J. R. Meteorol. Soc.*, **137**, 1-28.
- Giese, B. S., H. F. Seidel, G. P. Compo, and P. D. Sardeshmukh (2016) An ensemble of ocean reanalyses for 1815-2013 with sparse observational input. *J. Geophys. Res. Ocean.*, **121**, 6891-6910.
- Hirahara S., I. Masayoshi, and Y. Fukuda (2014) Centennial-scale sea surface temperature analysis and its uncertainty. *J. Climate*, **27**, 57-75.
- Kistler, R., E. Kalnay, W. Collins, S. Saha, G. White, J. Woollen, M. Chelliah, W. Ebisuzaki, M. Kanamitsu, V. Kousky, H. van den Dool, R. Jenne, and M. Fiorino (2001) The NCEP-NCAR 50-year reanalysis: monthly means CD-ROM and documentation. *Bull. Amer. Meteorol. Soc.*, **82**, 247-267.
- World Bank (1954) *Important factors in the world coffee market*. Technical operations project series, No. TO 53, Washington, D. C., World Bank Group.
- Kohlhepp, G. (1975) *Agrarkolonisation in Nord-Paraná. Wirtschafts- und sozialgeographische Entwicklungsprozesse einer randtropischen Pionierzone Brasiliens unter dem Einfluss des Kaffeeanbaus*. Steiner, Wiesbaden.
- Laloyaux, P., E. de Boissésou, and P. Dahlgren (2017) CERA-20C: An Earth system approach to climate reanalysis. *ECMWF Newsletter* **150**, 25-30.
- Laloyaux, P., M. Balmaseda, D. Dee, K. Mogensen, and P. Janssen (2016) A coupled data assimilation system for climate reanalysis. *Q. J. R. Meteorol. Soc.*, **142**, 65-78.
- Marengo, J., A. Cornejo, P. Satyamurty, C. Nobre, and W. Sea (1997) Cold Surges in Tropical and Extratropical South America: The Strong Event in June 1994. *Mon. Wea. Rev.*, **125**, 2759-2786.
- Marshall, C. F. (1983) *The World Coffee Trade*. Woodhead-Faulkner. Prentice-Hall, Upper Saddle River, New Jersey, USA. 254 pp.
- Pezza, A. B. and T. Ambrizzi (2005) Dynamical conditions and synoptic tracks associated with different types of cold surges over tropical South America. *Int. J. Climatol.*, **25**, 215-241.
- Poli, P., H. Hersbach, D. Dee, P. Berrisford, A. Simmons, F. Vitart, P. Laloyaux, D. Tan, C. Peubey, J.-N. Thépaut, Y. Trémolet, E. Holm, M. Bonavita, L. Isaksen, and M. Fisher (2016) ERA-20C: An Atmospheric Reanalysis of the Twentieth Century. *J. Clim.*, **29**, 4085-4097.
- Saha, S., S. Moorthi, H.-L. Pan, X. Wu, J. Wang, S. Nadiga, P. Tripp, R. Kistler, J. Woollen, D. Behringer, H. Liu, D. Stokes, R. Grumbine, G. Gayno, J. Wang, Y.-T. Hou, H.-Y. Chuang, H.-M. H. Juang, J. Sela, M. Iredell, R. Treadon, D. Kleist, P. Van Delst, D. Keyser, J. Derber, M. Ek, J. Meng, H. Wei, R. Yang, S. Lord, H. Van Den Dool, A. Kumar, W. Wang, C. Long, M. Chelliah, Y. Xue, B. Huang, J.-K. Schemm, W. Ebisuzaki, R. Lin, P. Xie, M. Chen, S. Zhou, W. Higgins, C.-Z. Zou, Qu. Liu, Y. Chen, Y. Han, L. Cucurull, R. W. Reynolds, G. Rutledge, and M. Goldberg (2010) The NCEP Climate Forecast System Reanalysis. *Bull. Amer. Meteorol. Soc.*, **91**, 1015-1057.